# UAV Surveillance Under Visibility and Dwell-Time Constraints *

**Jeffrey R. Peters**†
Systems Department
United Technologies Research Center
East Hartford, CT 06118
Email: petersjr@utrc.utc.com

**Amit Surana**
Systems Department
United Technologies Research Center
East Hartford, CT 06118
Email: suranaa@utrc.utc.com

**Grant S. Taylor**
Aviation Development Directorate
United States Army
Moffett Field, CA, 94035-1000

**Terry S. Turpin**
Aviation Development Directorate
United States Army
Moffett Field, CA, 94035-1000

**Francesco Bullo**
Department of Mechanical Engineering
University of California
Santa Barbara, CA 93106
Email: bullo@engr.ucsb.edu

A framework is introduced for planning unmanned aerial vehicle flight paths for visual surveillance of ground targets, each having particular viewing requirements. Specifically, the framework is designed for instances in which each target is associated with a set of imaging parameters, including a desired (i) tilt angle, (ii) azimuth, with the option of a 360-degree view, and (iii) dwell-time. Tours are sought to image the targets, while minimizing both the total mission time and the time required to reach the initial target. An $\epsilon$-constraint scalarization is used to pose the multi-objective problem as a constrained optimization, which, through careful discretization, can be approximated as a discrete graph-search. It is shown that, in many cases, this approximation is equivalent to a generalized traveling salesperson problem. A heuristic procedure for solving the discrete approximation and recovering solutions to the full routing problem is presented and illustrated through numerical studies.

*DISTRIBUTION A. Approved for public release: distribution unlimited (PR #3688). This work has been sponsored by the U.S. Army Research Office and the Regents of the University of California, through Contract Number W911NF-09-D-0001 for the Institute for Collaborative Biotechnologies, and that the content of the information does not necessarily reflect the position or the policy of the Government or the Regents of the University of California, and no official endorsement should be inferred.

†Corresponding author

## 1 Introduction

### 1.1 Overview

The use of autonomous mobile sensors is becoming increasingly common in civilian and military applications. Tasks that can benefit from autonomous sensors include search and rescue, forest fire or oil spill monitoring, surveillance and reconnaissance, transportation and logistics management, and hazardous waste cleanup [1, 2, 3]. These applications require intelligent and practical strategies to govern autonomous behavior in the presence of numerous constraints that arise in realistic missions.

This technical brief considers a particular mobile sensor scenario that is of interest in many applications, e.g., in military operations [4], where a single fixed-wing Unmanned Aerial Vehicle (UAV) collects visual sensor data within a large environment. Here, the UAV is equipped with a gimbaled camera, and must provide surveillance imagery of multiple, static ground targets, each having associated imaging constraints. These pre-specified constraints include (i) a desired tilt angle with tolerances, (ii) a desired azimuth with tolerances, including the option of a 360-degree view, and (iii) the amount of time that the UAV should dwell before moving to the next target. The goal is to construct flight paths that are optimal in some sense, while simultaneously allowing each target to be imaged to specification.

Ideally, our framework seeks flight paths that simultaneously minimize two metrics: (i) the time required for the UAV to image all targets and return to the initial target, and

(ii) the delay between the mission onset and the time the UAV reaches its first target. The latter goal is motivated primarily by operational scenarios in which mission critical planning cannot progress until initial sensory information is collected, e.g., this arises in military reconnaissance missions where sensory data supports the operations of a manned aircraft [5].

Since these two objectives are conflicting in general, we construct solutions by constraining the second performance metric and optimizing over the first, consistent with standard *scalarization* approaches for addressing multi-objective problems [6]. We develop a discrete-approximation strategy for constructing high-quality solutions to the scalarized problem, naturally leading to a complete heuristic framework for the full, multi-objective mission.

Specifically, this brief proceeds as follows. First, we show how the multi-objective routing problem with both visibility and dwell-time constraints is posed as a constrained optimization problem through reasonable assumptions about UAV trajectories and dwell-time maneuvers. Then, we illustrate how the constrained optimization problem is approximated by a discrete problem, which implicitly considers both the time required for appropriate dwell-time maneuvers and the visibility constraints. Next, we present a novel heuristic method for solving the discrete approximation that leverages solutions to standard *Generalized Traveling Salesperson Problem* (GTSP) instances. Finally, we integrate these constructions into a complete framework to produce high-quality solutions to the full, multi-objective routing problem, and we illustrate these methods numerically.

### 1.2 Purpose and Scope

The primary purpose of this brief is two-fold. First, the presented approach serves to extend previous work relating to both discrete Dubins vehicle routing and set-based generalizations of TSPs, by explicitly incorporating dwell-time and visibility considerations within a multi-objective framework. More specifically, the problem herein is loosely interpreted as a generalization of both the *Polygon-Visiting Dubins Traveling Salesperson Problem (PVDTSP)* [7, 8] and the *Dubins Traveling Salesperson Problem with Neighborhoods (DTSPN)* [9]. To incorporate multiple objectives and explicit imaging constraints, we adopt a strategy that is, in some sense, an extension of [7], in which the authors approximate solutions to a PVDTSP by discretizing regions of interest and posing the resulting problem as a *Generalized Traveling Salesperson Problem (GTSP)*, which can be solved using well-known methods, e.g., through transformation to a standard Asymmetric Traveling Salesperson Problem (ATSP) and subsequent use of heuristic solvers (see [7, 10]).

The second primary purpose of our work is to demonstrate how a complex, operationally relevant UAV surveillance problem, which includes user-enforced imaging constraints, can be placed into an optimization framework whose solutions are approximated by leveraging the solutions to standard combinatorial routing problems.

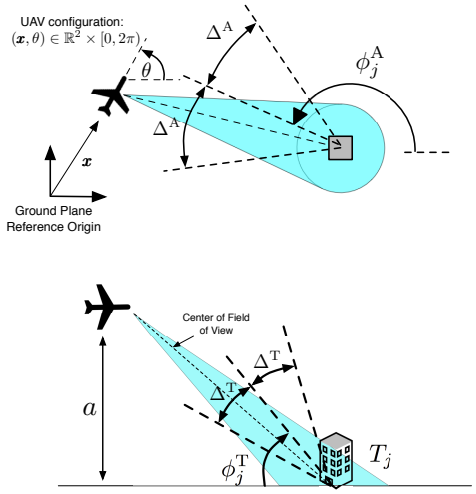


Fig. 1. Illustration of key imaging parameters associated target $T_j$.

## 2 Problem Formulation

### 2.1 UAV Specifications

Consider a single fixed-wing UAV, equipped with a GPS location device and a gimbaled camera. The camera is steered by a low-level controller, which is independent of the vehicle motion controller. We neglect the possibility of camera occlusions. The work herein focuses on high-level UAV trajectory planning, rather than low-level vehicle or camera motion control. We consider planar motion in a ground-plane reference frame, assuming the UAV maintains a fixed altitude $a$ and a fixed speed $s$. We model the UAV as a Dubins vehicle [11] with minimum turning radius $r$, neglecting dynamic effects caused by wind, etc. Let $\boldsymbol{v}_0 \in \mathbb{R}^2 \times [0, 2\pi)$ denote the UAV's initial configuration (location, heading).

### 2.2 Target Specifications

Consider $M$ static targets, each with associated imaging, i.e., visibility and dwell-time, requirements. Assume that the UAV must center each target within the camera's field of view for imaging, and thus no-two targets can be imaged simultaneously. The axis passing through the UAV location and the center of the camera field of view is used as a reference for assessing imaging constraints (see Figure 1).

Each target $T_j$ is associated a set of (fixed) parameters:

1. $\boldsymbol{t}_j \in \mathbb{R}^2$, the location of the target in the ground-plane,
2. $\texttt{BEH}_j \in \{\texttt{ANY}, \texttt{ANGLE}, \texttt{FULL}\}$, the required viewing behavior, where `ANY` indicates no preference for the azimuth of collected images, `ANGLE` indicates that the target should be imaged at a specific azimuth, and `FULL` indicates that a 360-degree view of the target be provided,
3. $\left[\phi_j^{\mathrm{A}} - \Delta_j^{\mathrm{A}}, \phi_j^{\mathrm{A}} + \Delta_j^{\mathrm{A}}\right] \subset \mathbb{R}$, a range of acceptable azimuths when $\texttt{BEH}_j = \texttt{ANGLE}$, as measured with respect to a reference ray in the ground plane (Fig. 1, top),
4. $\left[\phi_j^{\mathrm{T}} - \Delta_j^{\mathrm{T}}, \phi_j^{\mathrm{T}} + \Delta_j^{\mathrm{T}}\right] \subset (0, \frac{\pi}{2}]$, acceptable camera tilt angles as measured with respect to a plane parallel to the ground-plane (Fig. 1, bottom), and
5. $\tau_j \in \mathbb{Z}_{\geq 0}$, the required number of dwell-time "loops."

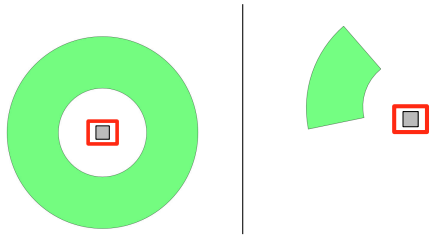

Fig. 2. An example visibility region $\texttt{VIS}_j$ when $\texttt{BEH}_j \neq \texttt{ANGLE}$ (left), and when $\texttt{BEH}_j = \texttt{ANGLE}$ (right).

Define the *visibility region*, $\texttt{VIS}_j \subset \mathbb{R}^2$, for target $T_j$ as the set of locations from which the UAV can image the target with an acceptable tilt angle and azimuth (that is, a tilt angle within the interval $\left[\phi_j^{\mathrm{T}} - \Delta_j^{\mathrm{T}}, \phi_j^{\mathrm{T}} + \Delta_j^{\mathrm{T}}\right]$ and, if $\texttt{BEH}_j = \texttt{ANGLE}$, an azimuth within the interval $\left[\phi_j^{\mathrm{A}} - \Delta_j^{\mathrm{A}}, \phi_j^{\mathrm{A}} + \Delta_j^{\mathrm{A}}\right]$; if $\texttt{BEH}_j \neq \texttt{ANGLE}$, then any azimuth is acceptable). Each $\texttt{VIS}_j$ is uniquely defined by the UAV altitude $a$, the location $\boldsymbol{t}_j$, the behavior $\texttt{BEH}_j$, and the intervals $\left[\phi_j^{\mathrm{T}} - \Delta_j^{\mathrm{T}}, \phi_j^{\mathrm{T}} + \Delta_j^{\mathrm{T}}\right]$, $\left[\phi_j^{\mathrm{A}} - \Delta_j^{\mathrm{A}}, \phi_j^{\mathrm{A}} + \Delta_j^{\mathrm{A}}\right]$. Algorithm 1 presents the methodology for constructing visibility regions. Note that, if $\texttt{BEH}_j \neq \texttt{ANGLE}$, then $\texttt{VIS}_j$ is a full annulus; otherwise, $\texttt{VIS}_j$ is an annular sector (Fig. 2). Fixing target locations, each visibility region is parameterized by two radii (lower, upper radial limits) together with two angles (lower, upper angular limits).

**Algorithm 1:** *Visibility Region Construction*

**Input** : a; $\phi_j^{\mathrm{T}}$, $\phi_j^{\mathrm{A}}$, $\Delta_j^{\mathrm{T}}$, $\Delta_j^{\mathrm{A}}$ for each $j \in \{1, \ldots, M\}$
**Output** : $\{\texttt{VIS}_j\}_{j\in\{1,\ldots,M\}}$

**for** *Each* $T_j$ **do**
  **if** $\texttt{BEH}_j \neq \texttt{ANGLE}$ **then**
1  Define $\texttt{VIS}_j$ as the annulus in $\mathbb{R}^2$ centered at $\boldsymbol{t}_j$ with radial limits $a / \tan(\phi_j^{\mathrm{T}} \pm \Delta_j^{\mathrm{T}})$
  **else**
2  Define $\texttt{VIS}_j$ as the annular sector in $\mathbb{R}^2$ centered at $\boldsymbol{t}_j$ with radial limits $a / \tan(\phi_j^{\mathrm{T}} \pm \Delta_j^{\mathrm{T}})$, and angular limits equivalent to $\phi_j^{\mathrm{A}} \pm \Delta_j^{\mathrm{A}}$.
3 **return** $\{\texttt{VIS}_j\}_{j\in\{1,\ldots,M\}}$

The variable $\tau_j \in \mathbb{Z}_{\geq 0}$ indicates the number of dwell-time "loops" that are required at $T_j$: If $\tau_j = 0$, then the UAV accomplishes its task by passing over any point within $\texttt{VIS}_j$. If $\tau_j > 0$, i.e., non-trivial dwell time is specified, assume the UAV images $T_j$ as follows: If $\texttt{BEH}_j = \texttt{FULL}$, the UAV makes $\tau_j$ full circles around the target location at some constant radius; if $\texttt{BEH}_j \neq \texttt{FULL}$, then the UAV selects a pivot point within $\texttt{VIS}_j$ and makes $\tau_j$ circles about the selected point at radius $r$. Each non-trivial dwell-time maneuver must be performed entirely within the appropriate visibility region. Fig. 3 shows examples of acceptable imaging behavior for various choices of $\tau_j$ and $\texttt{BEH}_j$. For the remaining analysis, assume that imaging parameters are chosen to ensure problem feasibility, i.e., there exists at least 1 dwell-time maneuver at each target satisfying the aforementioned constraints.

### 2.3 Problem Statement

The goal is to construct an optimal UAV trajectory with the following characteristics: The UAV begins its tour by moving from its initial configuration to a configuration where it can begin imaging a target and, after the initial maneuver, the UAV follows a closed trajectory, along which it images each target to specification. Note that separating the initial maneuver from the remaining closed route ensures that the target imaging behavior can be effectively repeated if desired. Recall the performance metrics to be minimized: (i) the time required for the UAV to traverse the closed portion of the generated trajectory (beginning and ending at the first target), and (ii) the time required for the UAV to perform its initial maneuver, i.e., move from $\boldsymbol{v}_0$ to the starting point of the closed portion. We consider the following problem.

**Problem 1 (Optimal UAV Tour).** *Find a UAV tour (consisting of an initial maneuver, and a closed trajectory) that solves the following optimization problem:*

$$\begin{aligned} &\textit{Minimize:} && \textit{Closed Trajectory Time},\\ &\textit{Subject To:} && \textit{Initial Maneuver Time} \leq \epsilon,\\ &&& \textit{Dynamic Constraints Satisfied (Sec. 2.1), and}\\ &&& \textit{Correct Dwell-Time Maneuvers Performed}\\ &&&\quad \textit{at Each Target (Sec. 2.2),} \end{aligned} \tag{1}$$

*where $\epsilon \geq 0$ is a constant parameter.*

## 3 Discrete Approximation

Problem 1, which explicitly considers all imaging constraints, is typically difficult to solve directly. However, by carefully sampling the UAV configuration space, we pose a discrete alternative whose optimal solutions approximate those of Problem 1. This discrete approximation is closely related to standard path-finding problems, allowing the use of existing solvers to produce high-quality sub-optimal solutions. This section develops the discrete problem of interest.

### 3.1 Configuration Space Sampling

We sample the UAV configuration space to obtain a finite collection of points of the form $\boldsymbol{v} \coloneqq (\boldsymbol{x}, \theta) \in \mathbb{R}^2 \times [0, 2\pi)$. These points serve as the basis for the discrete approximation to Problem 1. Specifically, we choose a set of points that each represent the starting and ending configuration of an appropriate dwell-time "loop" at some target. That is, each sampled point $\boldsymbol{v} \coloneqq (\boldsymbol{x}, \theta)$ has heading $\theta$ that points in a direction tangent to a valid dwell-time loop (associated with target $\texttt{TAR}_{\boldsymbol{v}}$) passing through location $\boldsymbol{x} \in \texttt{VIS}_j$. By pairing each $\boldsymbol{v}$ with its target $\texttt{TAR}_{\boldsymbol{v}}$, this procedure creates a natural one-to-one mapping between the generated points and a set of feasible dwell-time maneuvers. As such, subsequent graph formulations can "disregard" dwell-time constraints by using an augmented graph distance. Fig. 4 shows examples of valid sampled sets associated with some $T_j$. Here, the dot is the point's location and the arrow represents its heading.

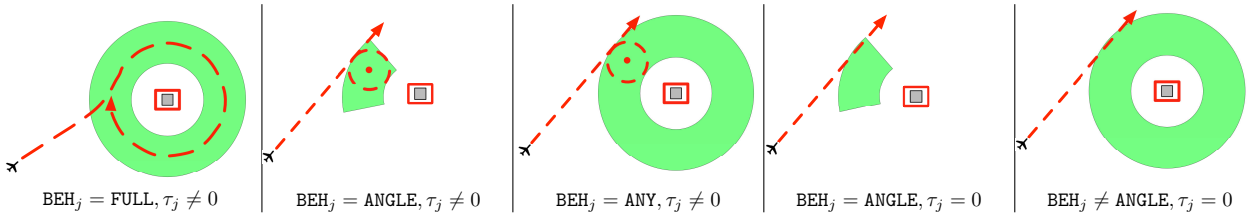


Fig. 3. Example imaging behaviors at target $T_j$ for various choices of $\mathtt{BEH}_j$ and $\tau_j$.

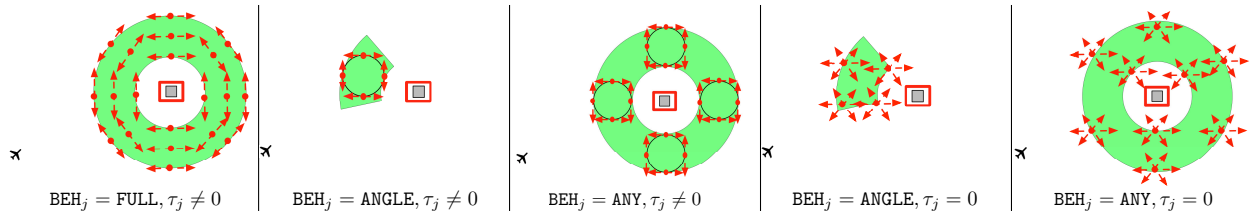


Fig. 4. Examples of valid configuration samples associated with $T_j$ for various choices of $\mathtt{BEH}_j$ and $\tau_j$.

Algorithm 2 outlines the sampling process. Here, $N \in \mathbb{N}$ is a parameter representing the number of sample points associated with each target, $V$ is the resultant set of sampled UAV configurations, and each set $\mathtt{DWL}_j$ is defined thusly: If $\tau_j \neq 0$, let $\mathtt{DWL}_j$ be the set of points $\boldsymbol{v} := (\boldsymbol{x}, \theta) \in \mathtt{VIS}_j \times [0, 2\pi)$ having location $\boldsymbol{x}$ that lies on the circular image of an appropriate dwell-time maneuver and heading $\theta$ that points in a direction tangent to the same circular image at $\boldsymbol{x}$. If $\tau_j = 0$, let $\mathtt{DWL}_j := \mathtt{VIS}_j \times [0, 2\pi)$. Note that, since all valid dwell-time loops associated with some target passing through a point $\boldsymbol{v} \in V$ have the same radii, we can assume without loss of generality that each $\boldsymbol{v}$ is the starting/ending configuration of a single loop associated with $\mathtt{TAR}_{\boldsymbol{v}}$.

**Algorithm 2:** *Configuration Space Sampling*

**Input** : $N \in \mathbb{N}$; $a$; $\mathtt{VIS}_j, \tau_j$ for all $j \in \{1, \ldots, M\}$
**Output** : $V$, $\{\mathtt{TAR}_{\boldsymbol{v}}\}_{\boldsymbol{v} \in V}$

Initialize $V = \emptyset$;
**for** *Each* $T_j$ **do**
  Construct and parameterize $\mathtt{DWL}_j$ by considering the images of valid dwell-time maneuvers at target $T_j$;
  **for** $k \in \{1, \ldots, N\}$ **do**
    Sample $\boldsymbol{v}_k \in \mathtt{DWL}_j$, associate the target $T_j$ to $\boldsymbol{v}_k$, i.e., define $\mathtt{TAR}_{\boldsymbol{v}_k} := T_j$, and add $\boldsymbol{v}_k$ to $V$;
**return** $V$, $\{\mathtt{TAR}_{\boldsymbol{v}}\}_{\boldsymbol{v} \in V}$

### 3.2 Graph Construction

Given the set of sampled points $V$ that is returned by Algorithm 2, we utilize Algorithm 3 to construct a weighted, directed graph $G := (V \cup \{\boldsymbol{v}_0\}, E, W)$ that effectively discretizes the solution space of Problem 1. Here, the edge set $E$ contains directed edges connecting each pair of nodes in $V$, along with directed edges connecting the initial UAV configuration $\boldsymbol{v}_0$ with each node in $V$. Weights are defined via an augmented distance that includes both the time required to complete the dwell-time maneuver at the source node and the time required to travel between configurations. The discrete approximation to Problem 1 using the graph $G$ is presented in Problem 2.

**Problem 2 (Discrete Approximation).** *Consider the graph* $G := (V \cup \{\boldsymbol{v}_0\}, E, W)$ *resulting from Algorithm 3. Find a sequence* $\boldsymbol{v}_1, \boldsymbol{v}_2, \ldots, \boldsymbol{v}_M \in V$ *that solves*

$$\begin{aligned} &\textit{Minimize:} && W(\boldsymbol{v}_M, \boldsymbol{v}_1) + \sum_{k=1}^{M-1} W(\boldsymbol{v}_k, \boldsymbol{v}_{k+1}) \\ &\textit{Subject To:} && W(\boldsymbol{v}_0, \boldsymbol{v}_1) \leq \epsilon, \textit{ and} \\ &&& \mathtt{TAR}_{\boldsymbol{v}_{k_1}} \neq \mathtt{TAR}_{\boldsymbol{v}_{k_2}}, \textit{ for any } k_1 \neq k_2, \end{aligned} \tag{2}$$

*where* $\boldsymbol{v}_0$ *corresponds to the initial UAV configuration and* $\epsilon \geq 0$ *is a constant parameter.*

**Algorithm 3:** *Graph Construction*

**Input** : $N \in \mathbb{N}$; $V$, $\{\mathtt{TAR}_{\boldsymbol{v}}\}_{\boldsymbol{v} \in V}$; $\boldsymbol{v}_0$, $s$, $a$, $r$
**Output** : $G := (V \cup \{\boldsymbol{v}_0\}, E, W)$

Initialize the edge set $E = \emptyset$;
**for** *Each pair of distinct points* $\boldsymbol{v}_{k_1}, \boldsymbol{v}_{k_2} \in V$ **do**
  Add the directed edges $(\boldsymbol{v}_{k_1}, \boldsymbol{v}_{k_2})$ and $(\boldsymbol{v}_{k_2}, \boldsymbol{v}_{k_1})$ to $E$;
  Set the weight $W(\boldsymbol{v}_{k_1}, \boldsymbol{v}_{k_2})$ equal to the sum of:
    (i) the time required to perform the dwell-time maneuver associated with $\boldsymbol{v}_{k_1}$, and
    (ii) the time required to traverse the optimal Dubins path from $\boldsymbol{v}_{k_1}$ to $\boldsymbol{v}_{k_2}$;
  Set the weight $W(\boldsymbol{v}_{k_2}, \boldsymbol{v}_{k_1})$ equal to the sum of:
    (i) the time required to perform the dwell-time maneuver associated with $\boldsymbol{v}_{k_2}$, and
    (ii) the time required to traverse the optimal Dubins path from $\boldsymbol{v}_{k_2}$ to $\boldsymbol{v}_{k_1}$;
Add the initial UAV configuration $\boldsymbol{v}_0$ to the node set of $G$;
**for** *Each node* $\boldsymbol{v} \in V$ **do**
  Add the directed edges $(\boldsymbol{v}_0, \boldsymbol{v})$ to $E$;
  Set the weight $W(\boldsymbol{v}_0, v)$ equal to the time required to traverse the optimal Dubins path from $\boldsymbol{v}_0$ to $\boldsymbol{v}$;
**return** $G = (V \cup \{\boldsymbol{v}_0\}, E, W)$

## 4 UAV Tour Construction

Notice that solutions to Problem 1 can be recovered from solutions to Problem 2. Indeed, given a solution

$\boldsymbol{v}_1, \ldots, \boldsymbol{v}_M$ to (2), we recover a feasible solution to (1) by: (i) concatenating the optimal Dubins paths between adjacent nodes in the sequence (also appending the path from $\boldsymbol{v}_0$ to $\boldsymbol{v}_1$ at the beginning and the path from $\boldsymbol{v}_M$ with $\boldsymbol{v}_1$ at the end) and (ii) appending the dwell-time trajectory associated to each node $\boldsymbol{v}_1, \ldots, \boldsymbol{v}_M$. The remainder of our analysis studies the discrete approximation (Problem 2) and its relation to the continuous formulation (Problem 1).

### 4.1 Solving the Discrete Problem

We leverage solutions of a classic graph path-finding problem to find solutions to (2). In particular, we propose a heuristic framework that relates solutions of (2) the following *Generalized Traveling Salesperson Problem* (GTSP).

**Problem 3 (GTSP).** *Given a complete, weighted, directed graph $\mathcal{G} := (\mathcal{V}, \mathcal{E}, \mathcal{W})$, and a family of finite, non-empty subsets $\{\mathcal{V}_j \subseteq \mathcal{V}\}_{j \in \{1,\ldots,M\}}$, find a minimum weight, closed path that visits exactly one node from each subset $\mathcal{V}_j$.*

Problem 2 is *not* equivalent to a GTSP in general, due to the constraint on the initial maneuver. However, GTSP solution procedures can be leveraged in constructing solutions to the constrained problem. Indeed, a heuristic procedure for constructing solutions to Problem 2 using the solutions to related GTSP instances is outlined in Algorithm 4. Here, $\texttt{INL}_\epsilon$ denotes the set of all nodes in $V$ that can be reached from $\boldsymbol{v}_0$ in time less than $\epsilon$.

**Algorithm 4:** *Heuristic Solution to Problem 2*

**Input** : $G = (V \cup \{\boldsymbol{v}_0\}, E, W)$, $\{\texttt{TAR}_{\boldsymbol{v}}\}$
**Output** : $\boldsymbol{v}_1, \ldots, \boldsymbol{v}_M$

Construct the set $\texttt{INL}_\epsilon := \{\boldsymbol{v} \in V \mid W(\boldsymbol{v}_0, \boldsymbol{v}) \leq \epsilon\}$;
**if** *$\texttt{INL}_\epsilon$ is empty* **then**
  **return** "Problem 2 Infeasible"
**else**
  Select a subset $\texttt{INL}^*_\epsilon \subseteq \texttt{INL}_\epsilon$, whose elements are all associated with a single target $T_{\hat{\jmath}}$;
  Construct the subgraph $\mathcal{G} := (\mathcal{V}, \mathcal{E}, \mathcal{W}) \subseteq G$ that is induced by the node set $\mathcal{V} \subseteq V$, where $\mathcal{V} := V \backslash \{\boldsymbol{v} \in V \mid \texttt{TAR}_v = T_{\hat{\jmath}}, v \notin \texttt{INL}^*_\epsilon\}$;
  Formulate and solve the GTSP (Problem 3) using the graph $\mathcal{G}$ and subsets $\mathcal{V}_j := \{\boldsymbol{v} \in \mathcal{V} \mid \texttt{TAR}_v = T_j\}$;
  Define $\boldsymbol{v}_1, \boldsymbol{v}_2, \ldots, \boldsymbol{v}_M$ as the unique, circular shift[1] of the resultant GTSP solution that satisfies $\texttt{TAR}_{\boldsymbol{v}_1} = T_{\hat{\jmath}}$;
  **return** $\boldsymbol{v}_1, \ldots, \boldsymbol{v}_M$

### 4.2 Complete Tour Construction

The complete procedure is presented in Algorithm 5. Solutions produced by Algorithm 5 are not optimal in general, though they will exhibit structural characteristics that generally improve in quality (with respect to Problem 1) as the sampling granularity is made increasingly fine. We omit a full mathematical characterization of limiting behavior in this brief and simply note that properties related to *resolution completeness* can be rigorously shown.

[1] A *circular shift* of an ordered sequence $a_1, a_2, \ldots, a_M$ is an ordered sequence $a_i, a_{i+1}, \ldots, a_M, a_1, \ldots, a_{i-1}$, where $i \in \{1, \ldots, M\}$

**Algorithm 5:** *Heuristic Tour Construction via GTSPs*

**Input** : $\boldsymbol{v}_0, s, a, r; N \in \mathbb{N}; \{T_j\}_{j \in \{1,\ldots,M\}}$
**Output** : Complete UAV Route

*% Create visibility regions*;
Create target visibility regions via Algorithm 1.
*% Create the discrete approximation*;
Sample the configuration space and create the graph $G$ via Algorithms 2 and 3. Formulate Problem 2;
*% Solve the discrete approximation*;
Construct a solution $\boldsymbol{v}_1, \ldots, \boldsymbol{v}_M$ to Problem 2 via Algorithm 4;
**if** *Algorithm 4 returns an error (Problem 2 is infeasible)* **then**
  **return** "Error: Discrete Approximation Infeasible"
*% Convert the solution of Problem 2 into a solution to Problem 1*;
Construct the optimal Dubins path that visits the nodes in the following order: $\boldsymbol{v}_0, \boldsymbol{v}_1, \ldots, \boldsymbol{v}_M, \boldsymbol{v}_1$;
Append dwell-time maneuvers to recover a solution to Problem 1.;
**return** UAV Route: Initial Maneuver + Closed Trajectory

## 5 Numerical Examples

The presented algorithms are shown via numerical examples. For each example, solutions to Problem 1 are constructed via Algorithm 5, where GTSPs are solved through transformation into an equivalent ATSP (see [10]) that is subsequently solved using an implementation of the Lin-Kernighan heuristic. In all cases, the set $\texttt{INL}^*_\epsilon$ (Algorithm 4) is chosen as the set of all points in $\texttt{INL}_\epsilon$ associated with some single target. A slightly modified version of Algorithm 2 is used for sampling in which the number of samples, $N$, associated with each target is not fixed *a priori*, but instead is determined by creating a grid of samples within the sampling subsets. Grid spacing is determined by 3 parameters $\delta r$, $\delta\theta$, and $\delta\alpha$, which represent, loosely, the radial location spacing, the angular location spacing, and the angular heading spacing, resp. The parameters $\delta r$, $\delta\theta$, and $\delta\alpha$ are inversely proportional to the number of samples at each target.

### 5.1 Pareto-Optimal Front

The first example is a 5 target mission with the following UAV parameters: $r = 750$ m, $a = 1000$ m, $s = 39$ m/s, and $\boldsymbol{v}_0 = ((-2500, 500)\text{ m}, 0)$. Target parameters are shown in Table 1. The approximate Pareto-optimal front for Problem 1 as a function of the sampling granularity is shown in Figure 5. The figure also shows illustrations of solutions produced at spacing condition 5 when $\epsilon = 65$ s (left) and $\epsilon = 205$ s (right). The following steps were taken to generate each curve: First, Algorithm 5 was called for a series of $\epsilon$ values, and the resulting initial maneuver/closed trajectory times were recorded. Then, in post-processing, the approximate Pareto-optimal curve was generated by selecting, for each $\epsilon$, the lowest cost route satisfying the initial maneuver constraint. Note that increasing $\epsilon$ corresponds to relaxing the initial maneuver constraint, and thus the cost is non-increasing in $\epsilon$. Notice also that the Pareto-optimal fronts shift toward zero as the sampling spacing is decreased.

Table 1. Target Input Data

| $T_j$ | $t_j$ | $\mathtt{Beh}_j$ | $\tau_j$ | $\left[\phi_j^{\mathrm{A}} - \Delta_j^{\mathrm{A}}, \phi_j^{\mathrm{A}} + \Delta_j^{\mathrm{A}}\right]$ | $\left[\phi_j^{\mathrm{T}} - \Delta_j^{\mathrm{T}}, \phi_j^{\mathrm{T}} + \Delta_j^{\mathrm{T}}\right]$ |
|---|---|---|---|---|---|
| $T_1$ | $(5000, -5000)$ m | FULL | 2 | – | $[\frac{\pi}{8}, \frac{3\pi}{8}]$ |
| $T_2$ | $(4300, -1750)$ m | ANGLE | 1 | $[\frac{\pi}{4}, \frac{3\pi}{4}]$ | $[\frac{\pi}{8}, \frac{3\pi}{8}]$ |
| $T_3$ | $(0, 4000)$ m | FULL | 3 | - | $[\frac{\pi}{8}, \frac{3\pi}{8}]$ |
| $T_4$ | $(-8000, -2000)$ m | ANY | 1 | - | $[\frac{\pi}{8}, \frac{3\pi}{8}]$ |
| $T_5$ | $(-2000, 8000)$ m | ANGLE | 0 | $[\frac{3\pi}{2}, 2\pi]$ | $[\frac{\pi}{8}, \frac{3\pi}{8}]$ |

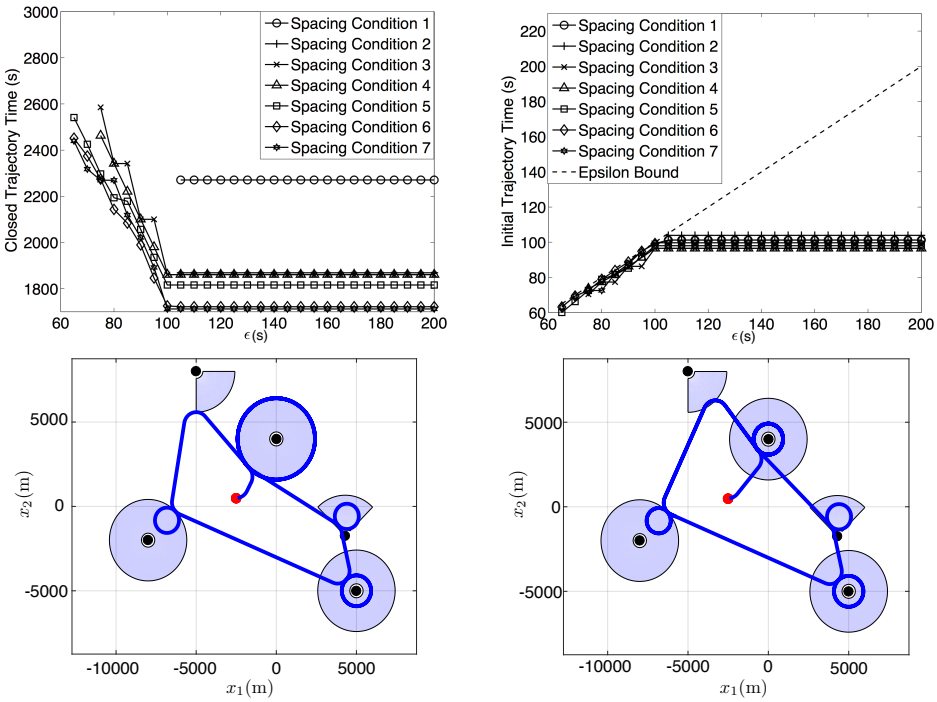


Fig. 5. Approximate Pareto-Optimal Front and Example Routes for the Spacing Conditions in Table 2

Table 2. Spacing Conditions

| Spacing Condition | $\delta r$ | $\delta\theta$ | $\delta\alpha$ |
|---|---|---|---|
| 1 | 1000 m | $\pi$ | $\pi$ |
| 2 | 500 m | $\pi$ | $\pi$ |
| 3 | 500 m | $\pi/2$ | $\pi/2$ |
| 4 | 250 m | $\pi/2$ | $\pi/2$ |
| 5 | 250 m | $\pi/4$ | $\pi/4$ |
| 6 | 125 m | $\pi/4$ | $\pi/4$ |
| 7 | 125 m | $\pi/8$ | $\pi/8$ |

### 5.2 Performance

The next example illustrates the performance of Algorithm 5 in comparison to an incremental, "greedy" alternative that operates as follows: Visibility region creation and configuration space sampling are done using Algorithms 1 and 2. Starting with the initial UAV configuration, each successive UAV destination is chosen by selecting the closest node (Dubins distance) associated with a target that has not yet been imaged. A valid route is constructed by appending dwell-time maneuvers and connecting the last selected configuration ($\boldsymbol{v}_M$) with the first ($\boldsymbol{v}_1$). We consider a 5 target mission with the same UAV parameters, target locations, imaging behaviors, and tolerances as in Section 5.1. However, we vary the number of dwell-time loops associated with each (each target requires same number of loops).

The difference between the closed trajectory times produced by the greedy method and those produced by Algorithm 5 as a function of $\epsilon$ under spacing condition 5 (Fig. 5) is shown in Fig. 6.Notice that the performance of the greedy search method can be made arbitrarily poor by increasing the number of dwell-time loops. This result is primarily due to targets that require a 360-degree view, since the greedy heuristic generally chooses points lying on the visibility region perimeter, which are very far from the target location. Thus, increasing the number of dwell-time loops can drasti-

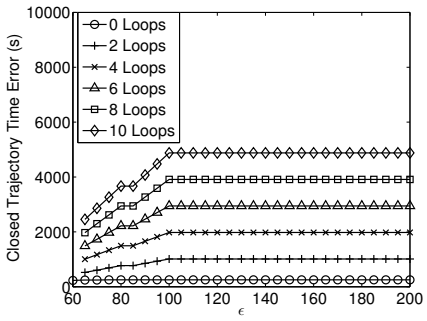


Fig. 6. Relative performance of the greedy algorithm.

cally increase total tour times. As such, Algorithm 5 can provide a significant advantage over similar incremental planning strategies when non-trivial dwell-times are required.

## 6 Conclusions

A straightforward algorithmic framework was presented for constructing unmanned aerial vehicle trajectories for surveillance of multiple targets, each having visibility and dwell-time constraints.

Avenues of future research include the expansion to the multi-vehicle case, explicit comparisons with other routing schemes (e.g., Markov chain-based schemes), and an investigation of alternative discretization strategies. Further, theoretical studies of the implications of subset selection in Algorithm 4 and other manipulations to aid computation are of interest. In addition, incorporation of uncertain dwell-times and the explicit pairing with other facets of complex missions, e.g. operator analysis of imagery, should be explored. Other valuable extensions include the explicit consideration of visual occlusions and the incorporation of more complex vehicle dynamics. Experimental validation of these approaches in an appropriately designed hardware testbed would also provide further insight into practical implementation of the presented algorithms.

## Acknowledgments

The authors thank Karl J. Obermeyer of Obermeyer Labs for his insight regarding vehicle routing.

## References

[1] Roberts, J., 2006. "Special issue on uninhabited aerial vehicles". *Journal of Field Robotics,* **23**(3–4).

[2] Valavanis, K. P., 2008. *Advances in Unmanned Aerial Vehicles: State Of The Art And the Road To Autonomy*. Springer.

[3] US Air Force, 2010. Report on technology horizons, a vision for Air Force Science And Technology during 2010–2030. Tech. rep., AF/ST-TR-10-01-PR, United States Air Force. Retrieved from http://www.defenseinnovationmarketplace.mil/ resources/ AF_TechnologyHorizons2010-2030.pdf on Feb. 8, 2016.

[4] US Office of the Secretary of Defense, 2005. Unmanned aircraft systems (UAS) roadmap, 2005-2030.

[5] Army, U., 2007. Attack reconnaissance helicopter operations. Tech. Rep. FM 3-04.126, Department of the Army (US), Feb. Retrieved from http://usacac.army.mil/sites/default/files/misc/doctrine/CDG/fms.html on Dec. 5, 2016.

[6] Miettinen, K., 1998. *Nonlinear Multiobjective Optimization*. Springer.

[7] Obermeyer, K. J., Oberlin, P., and Darbha, S., 2012. "Sampling-based path planning for a visual reconnaissance UAV". *AIAA Journal of Guidance, Control, and Dynamics,* **35**(2), pp. 619–631.

[8] Obermeyer, K., 2009. "Path planning for a uav performing reconnaissance of static ground targets in terrain". In AIAA Guidance, Navigation, and Control Conference, pp. 10–13.

[9] Isaacs, J., and Hespanha, J. P., 2013. "Dubins traveling salesman problem with neighborhoods: A graph-based approach". *Algorithms,* **6**(1), pp. 84–99.

[10] Noon, C. E., and Bean, J. C., 1991. "A Lagrangian based approach for the asymmetric generalized traveling salesman problem". *Operations Research,* **39**(4), pp. 623–632.

[11] Dubins, L. E., 1957. "On curves of minimal length with a constraint on average curvature and with prescribed initial and terminal positions and tangents". *American Journal of Mathematics,* **79**, pp. 497–516.